Nonresonant dielectric hole-burning spectroscopy on a titanium-modified lead magnesium niobate ceramic

O. Kircher, G. Diezemann, and R. Böhmer
Institut für Physikalische Chemie, Johannes Gutenberg-Universität, 55099 Mainz, Germany
(Received 5 December 2000; published 2 July 2001)

Nonresonant dielectric hole-burning experiments were performed on the titanium-modified relaxor ferroelectric lead magnesium niobate around the diffuse maximum in the dielectric permittivity. After applying large alternating electric pump fields we monitored the polarization response to small field steps for times between 0.3 ms and 100 s. Depending on the frequency of the pump oscillation a speedup of the polarization response was observed with a maximum located around times corresponding to the inverse pump frequency. The refilling of the dielectric holes was investigated for several temperatures, pump frequencies, and pump field amplitudes. It proceeded always slower than the time scale set by the pump frequencies. Additionally, we observe a significant increase of the refilling times for increasing pump field amplitudes. This finding can be interpreted to indicate that increasingly large pump fields enable the domain walls to cross larger and larger pinning barriers. The subsequent recovery process, which leads back to the equilibrium domain size distribution, proceeds in the absence of an external electrical field. This rationalizes that recovery is slowed down significantly by application of large pump field amplitudes since then the pinning barriers that have to be traversed back are larger.

DOI: 10.1103/PhysRevB.64.054103 PACS number(s): 77.22.Ej, 77.80.Dj, 77.84.Dy

I. INTRODUCTION

The complex perovskite lead magnesium niobate (PMN) is the prototypic substance belonging to the class of relaxor ferroelectrics (relaxors). Forty years after its discovery in 1958 by Smolenskii and Agronovskaja[1] the dielectric relaxation mechanism of PMN as well as other relaxors continues to be a point of discussion. On the one hand, relaxors are suitable for many technical applications. Because of their dielectric and piezoelectric properties they are commonly used as multilayer ceramic capacitors[2] and electromechanical actuators.[3] On the other hand, despite numerous experimental investigations the microscopic origin of the unusual physical properties of relaxors is still not clear. As compared to pure ferroelectric materials relaxors show an extremely broad permittivity versus temperature peak. This is often designated as ''diffuse'' phase transition. For relaxors the temperature of the maximum dielectric permittivity and loss exhibit a pronounced frequency dependence. Furthermore, a strong frequency dispersion of the permittivity below the peak and the absence of a Curie-Weiss behavior above are usually observed.[4,5]

Several investigations of the structural ordering of PMN yielded evidence for short-range, nonstoichiometric 1:1 ordering of the Mg^{2+} and Nb^{5+} cations on the *B* sites of the perovskite lattice[6,7] leading to strong space charges. As a consequence the crystal is split up into nanometer size regions with well defined local spontaneous polarization. The development of a long-range ferroelectric order is inhibited by the disorder.

In the past different models have been proposed to explain the dynamic properties of PMN-like relaxors. In the superparaelectric model introduced by Cross[4] the relaxor is considered as an ensemble of noninteracting polar regions each of them behaving like a conventional ferroelectric material. Another model[8–10] treats relaxors more like a glassy system with the well-known features of spin or dipole glasses.[11,12] In this model the polar regions show strong interactions leading to a frozen state at low temperatures characterized by random local orientations of the polarization. Several authors[13,14] argued in favor of random fields originating from quenched disorder which prevents a phase transition into a ferroelectrically ordered state. Glazounov *et al.*[15] described the dipolar dynamics in relaxor materials as a domain-wall motion (''breathing'') in a multidomain state. Very recently, Blinc *et al.*[16] established a random-bond random-field model for relaxors which combines features of a dipole glass with those of a random-field dominated scenario.

Up to now the question remains open whether these relaxors show (i) a ferroelectriclike state consisting of microsized nanodomains constrained by the quenched disorder or (ii) a glasslike freezing similar to the behavior in dipole glasses, however, with randomly interacting polar nanoregions. In scenario (i) the dipolar dynamics is governed by the depinning of domain walls. Domain walls in random systems are either formed through slowly decaying metastable configurations or competing interactions. For instance, in magnetic systems there is a competition between the stray field energy and the domain-wall energy.[17] As the structure evolves to a more stable state (or even to equilibrium) in response to an external perturbation the domain walls move in such a way that energetically more favorable domains grow at the expense of less favorable ones. The mobility of domains in random systems is often strongly reduced by pinning of the domain walls due to impurities or disorder effects.[18]

However, within both scenarios local random fields originating from charge imbalance play a major role. To decide which one of these approaches is the more realistic one linear dielectric measurement techniques are apparently not suit-

able. In some glassy systems not the linear dielectric permittivity but all higher nonlinear components $\varepsilon'_{\mathrm{nl}}$ exhibit a critical behavior around the glass transition.[12,19] Therefore the analysis of nonlinear components of the dielectric susceptibility was exploited in recent years.[20–22]

In our studies we combined both linear and nonlinear aspects of dielectric spectroscopy. The dielectric polarization $P(t)$ of PMN was measured as the linear response to small electric field steps. Additionally, we applied large alternating electric pump fields. Subsequently, the time evolution of the modified polarization response $P^*(t)$ was measured. By subtracting $P(t)$ from $P^*(t)$ one obtains a difference signal ΔP which reflects the effect caused by the pump process. With this method of dielectric nonresonant spectral hole-burning (NHB)[23] we are able to distinguish between subensembles responding at different time scales and to monitor their temporal evolution.[24]

Recently NHB was also successfully used to investigate spin glasses[25] and doped quantum paraelectrics[26] which show similar features to relaxor ferroelectrics.

II. MODELS FOR DIELECTRIC HOLE BURNING

In the following we describe two models for dielectric hole-burning. A simple approach to describe dipolar relaxational processes are electric dipoles in an asymmetric double-well potential (ADWP). This model is suited to describe several features of nonresonant dielectric hole-burning experiments.

For a given asymmetry Δ and barrier height V of an ADWP—where the asymmetry is defined as the difference between the minima of the two wells—the relaxation time τ is given by

$$\tau = \frac{1}{w_{12}+w_{21}} = \tau_0 \frac{\exp(V/k_BT)}{\cosh(\Delta/2k_BT)}. \tag{1}$$

Here w_{ij} is the transition rate from well i to well j and τ_0^{-1} is called the attempt frequency. The polarization of the double well results from the difference of the occupation numbers N_i and N_j of wells i and j. To ensure that without applying an external electric field no polarization is observed one can add the contributions from two double wells with opposite asymmetries. Then one can calculate the modified polarization response ΔP after applying a pump field of the form $P_{\mathrm{pump}}(t) = P_{\mathrm{pump}} \sin(\Omega t)$.[27,28] Restricting the calculation to contributions up to second order in the pump and first order in the probe field amplitude P_{probe} one obtains for the phase cycle described in Sec. III

$$\Delta P(t,t_w) = C\varepsilon''(\Omega\tau)\varepsilon''(2\Omega\tau)\{1-\exp(-2\pi N/\Omega\tau)\} \times \frac{t}{\tau}\exp\{-(t+t_w)/\tau\}, \tag{2a}$$

$$C = \frac{3}{2} E_{\mathrm{probe}} E_{\mathrm{pump}}^2 \frac{N\mu^4}{40(k_BT)^3} \sinh^2(\Delta/2k_BT) \times \{1-\sinh^2(\Delta/2k_BT)\}. \tag{2b}$$

Here N denotes the number of cycles of the sinusoidal pump field. This expression shows that the modification is proportional to the square of the pump field amplitude and $\varepsilon''(\Omega\tau)$, that means to the absorbed energy. The waiting time between pump and probe procedure is denoted as t_w. For each relaxation time τ one finds that $\Delta P(t)$ is peaked at $t=\tau$. By introducing a sufficiently broad distribution of relaxation times $g(\tau)$ the polarization modification becomes sensitive to the burning frequency Ω.[27] From Eq. (2) it can also be seen that in the ADWP model the hole-burning signal ΔP vanishes for asymmetries $\Delta \to 0$.

By generalizing the ADWP model to more than two equilibrium states one gets a more realistic scenario for relaxor materials. For PMN it is supposed that electric dipoles can orient along the eight $\langle 111 \rangle$ directions of the cubic unit cell.[29] Instead of the asymmetry in the ADWP model one can introduce local random electric fields acting on the dipoles in the potential wells. These fields may exist due to the disorder in the relaxor material. One can show that within a multiwell potential affected by random fields the modified polarization response looks similar to Eq. (2) except for different prefactors.[30]

Previously for the analysis of the NHB results of supercooled liquids[31] and spin glasses[25] a so-called ''box model'' was used. Recently a detailed justification of this approach in terms of a mesoscopic mean-field model was put forward.[32,33] We briefly outline a very similar approach for the analysis of our data.

The pump process is assumed to selectively speed up distinct elements out of the relaxation time distribution with a maximum effect around $t \approx \Omega^{-1}$. Therefore the pump procedure can be described by multiplying the equilibrium relaxation times τ_i by a function $f_{\mathrm{pump}}(\Omega,\tau_i)$ to obtain the difference between equilibrium and modified responses:

$$\Delta\Phi(t) = \Phi(t) - \Phi^*(t) = \sum_i g_i\{\exp(-t/\tau_i) - \exp(-t/\tau_i^*)\}. \tag{3a}$$

Here the modified (accelerated) relaxation times are given by

$$\tau_i^* = f_{\mathrm{pump}}(\Omega,\tau_i)\cdot\tau_i. \tag{3b}$$

Starting from the modified response function one can calculate the recovery function of the spectral holes for increasing waiting time t_w. Within the ''box model'' spectrally distinguishable features (the ''boxes'') are characterized by different nonthermodynamic ''fictive'' temperatures $T_{f,i}$. The Tool-Narayanaswamy[34] equation provides a connection of the change in the fictive temperature $\Delta T_{f,i}$ of the box ''i'' to the modified relaxation time τ_i^*:

$$\Delta T_{f,i} \approx k_B T^2 (\ln\tau_i - \ln\tau_i^*)/B. \tag{4}$$

Here T denotes the thermodynamic temperature and B an activation barrier. So the pump process leads to a small increase of the fictive temperature for the respective boxes. Assuming an exponential recovery of $T_{f,i}$ back to the thermodynamic temperature T,

$$\Delta T_{f,i}(t_w) = \Delta T_{f,i}(0)\exp(-t_w/\tau_i), \tag{5}$$

one can calculate the time evolution of the modified relaxation times τ_i^*. This allows us to compute the recovery function which is defined as the t_w-dependent maximum of the difference of the response functions Φ and Φ^*. It is given by

$$\Delta\Phi(t_w) = \Phi(\tau_i) - \Phi^*(\tau_i^*, t_w). \tag{6}$$

For each box it is assumed that the modification recovers to equilibrium with the equilibrium relaxation time τ_i of the corresponding box, i.e., $\Delta\Phi$ exhibits the same waiting time dependence like ΔP for a single ADWP [Eq. (2a)].

III. EXPERIMENTAL SETUP AND SAMPLE CHARACTERIZATION

We investigated crystalline ceramics of PMN with a nominal admixture of 10% $PbTiO_3$ (PT) provided by the Material Research Laboratory (Pennsylvania State University). They belong to the family of $A(B'_xB''_{1-x})O_3$ perovskite structure relaxors. The PMN-10PT material was found to be much less susceptible to chemical aging than the pure relaxor PMN, but, nevertheless, retains typical relaxor properties.[4,35] It has been observed that with increasing concentration of $PbTiO_3$ the presence of the Ti^{4+} ions suppresses the tendency of a 1:1 ordering of the Mg^{2+} and Nb^{5+} cations at the B site of the lattice.[6] The dimensions of the coin-shaped samples were $154\,mm^2 \times 1.3\,mm$ and $91.6\,mm^2 \times 0.8\,mm$, respectively. The surfaces were electroded with gold.

Prior to each measurement the specimens were annealed at 375 K for at least 30 min. This time turned out to be enough so that the thermal history of earlier experiments did not have any effect on the measured properties.[36] A common feature of mixed ferroelectrics, especially for thin films, is the problem of fatigue. For the electric-field sequences we used to investigate PMN-10PT we did not have this problem. For a ceramic sample of PLZT 8/65/35—a relaxor behaving similar to PMN-10PT—it has been shown[37] that fatigue is observable for more than 10^4 electric-field cycles with amplitudes of more than 250 kV/cm.

Each PMN-10PT sample was characterized using standard dielectric techniques. For frequencies from 20 Hz to 1 MHz we used an HP 4284A LCR meter. A cooling rate of 0.4 K/min was chosen for the whole temperature range. For lower frequencies $100\,mHz < \upsilon < 20\,Hz$ we employed a Solatron1260 Gain-Phase Analyzer equipped with an additional current-to-voltage interface.[38] The amplitudes of the driving electric fields did not exceed 10 V/cm in order to avoid nonlinear effects. During these measurements the PMN-10PT sample was thermostatted in a closed-cycle refrigerator system with a temperature stability better than ± 0.01 K.

For the pulsed dielectric spectroscopy and the nonresonant hole-burning experiments we generated electrical-field sequences by a computer-controlled digital/analog-converter which drives a fast high-voltage amplifier. The polarization of the PMN-10PT sample was detected by measuring the voltage across a reference capacitor in a modified Sawyer-Tower circuit. This voltage was amplified using a high-impedance circuit based on the operational amplifier AD 549JH and finally acquired with an analog/digital-data acquisition card for times ranging from about 0.3 ms to 100 s.[31] The timing of the field sequences for NHB was as follows: During a pumping time t_p one period of a sinusoidal electric field $E_{\mathrm{pump}}\sin(\Omega t)$ was applied across the sample. After a waiting time t_w the polarization was monitored as the response function to a dc electric field in the linear response regime. In order to eliminate unwanted effects in the polarization generated by the pump process suitable phase cycling was performed.[31] The modified polarization response is called $P^*(t)$ in the following. Together with the equilibrium polarization response $P(t)$, the difference signal was obtained as

$$\Delta P(t) = P^*(t) - P(t). \tag{7}$$

The equilibrium response $P(t)$ was received by applying a voltage step $U_{\mathrm{probe}} = E_{\mathrm{probe}}/d$ without pumping. Most of the experiments were carried out at a temperature of 275 K. Here the dielectric loss peaks at a frequency of 0.06 Hz. This corresponds to a time scale of 2.7 s, which provides a convenient scale in relation to the spectral range accessible with our present time-domain apparatus. Repetition times of 240–480 s between two subsequent field sequences were found to be long enough, so that the resulting difference polarization is not affected by the previous field sequence. In order to monitor the temperature dependence of the maximum spectral modifications and their re-equilibration times additional measurements were taken between 270 and 300 K.

IV. RESULTS AND ANALYSIS

A. Broadband and pulsed dielectric spectroscopy

Figure 1 shows the results from broadband dielectric spectroscopy. The temperature dependence of the dielectric permittivity ε', the dielectric loss ε'', and the loss factor $\tan\delta = \varepsilon''/\varepsilon'$ are plotted for different frequencies. The data reveal the typical relaxor peculiarities.[9,39] We found both a very large dielectric permittivity and a large dielectric loss. The permittivity and loss peak as a function of temperature are extremely broad. Their shape and their peak temperature exhibit strong frequency dispersion. For lower temperatures the dielectric loss is almost constant over at least seven decades in frequency. Coming from high temperatures, the phase angle $\tan\delta$ exhibits a pronounced increase and then reaches a frequency-dependent plateau.

By analyzing the polarization response $P(t)$ to small electric-field pulses a further characterization of the PMN-10PT sample was possible. The equilibrium polarization response generated by a constant step in the electric field shows a quasilogarithmic decay.[24] This renders it hard to extract a time scale of the decay. On the other hand, pulsed dielectric spectroscopy[40] is a suitable tool to map out a time scale τ in this situation. To do so, after a sufficiently long waiting time we applied a constant field for a pulse duration t_p (see inset of Fig. 2). After switching off the field the polarization $P(t)$ was monitored. Figure 2 shows the results for different durations t_p at a temperature of 275 K. It can be clearly seen that the average relaxation time

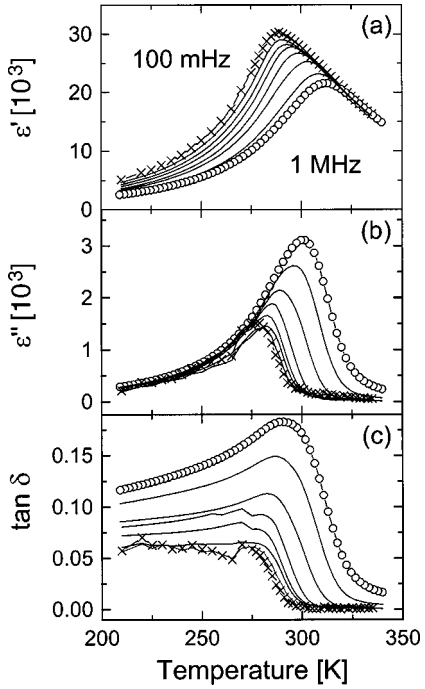

FIG. 1. Dielectric permittivity ε', dielectric loss ε'', and loss factor $\tan\delta=\varepsilon''/\varepsilon'$ for frequencies from 100 mHz (crosses) to 1 MHz (circles) and a field amplitude of 8 V/cm.

$$\langle\tau\rangle=\int_0^\infty P(t)/P(0)dt \tag{8}$$

of the polarization decay increases with longer t_p. For a pulse duration of about 10^4 s a plateau value is approached for $\langle\tau\rangle$. One of the possible interpretations of this finding[40] is that for shorter pulses the response function is dominated by the fast contributions of the distribution function. For long enough pulse durations all spectral features of the relaxation time distribution are addressed by the field so that the polarization decay proceeds with the equilibrium relaxation time at that temperature.

B. Frequency dependence of the modified response

NHB allows us to address differently relaxing subensembles in disordered dipolar substances. Figure 3(a) shows

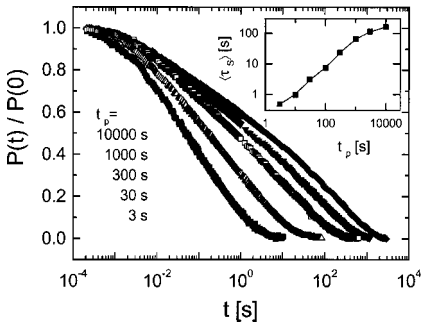

FIG. 2. Normalized polarization decay after applying a field pulse across the sample with a duration t_p ranging from 3 to 10 000 s. The electrical field was chosen to be 38.5 V/cm. The inset shows the mean relaxation times of the polarization decay calculated according to Eq. (8).

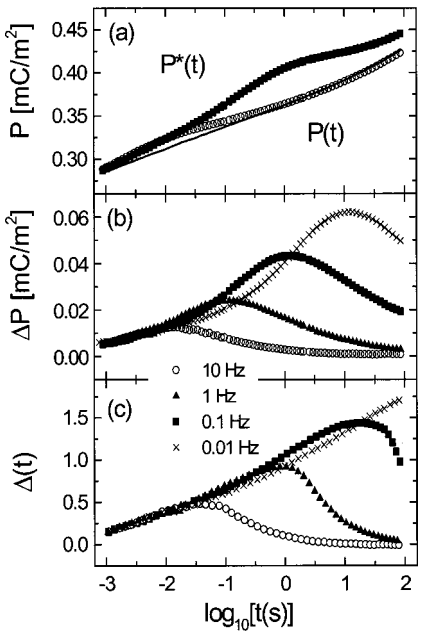

FIG. 3. (a) Polarization responses to a field step after pumping with a sinusoidal pump field of 231 V/cm (symbols) and without pumping (line). (b) Polarization modifications ΔP after pumping with the same pump field for pump frequencies of 10, 1, 0.1, and 0.01 Hz. (c) Difference along the time axis $\Delta(t)=\Delta\log_{10}(t)$ for the same data as in (b).

the step response function $P(t)$ and modified response function $P^*(t)$ for two different pump frequencies at a temperature of 275 K. Both $P(t)$ and $P^*(t)$ were measured as the polarization response to a constant probe field $E_{\text{probe}}=23.1$ V/cm. In the accessible time range $P(t)$ evolves in an almost logarithmic fashion. A similar behavior is often observed in the magnetization of spin glasses.[11] For PMN-10PT it indicates a broad distribution of dipolar reorientation times. The modified response function $P^*(t)$ was measured after applying one period of a sinusoidal pump field of the amplitude 231 V/cm. This leads to a modification of the relaxation spectrum which can be monitored as a speedup in the polarization response. The maximum in ΔP appears at a time $t_{\max}$ corresponding to the inverse pump frequency Ω^{-1}. In the following the maximum is denoted as $\Delta P_{\max}=\max|\Delta P(t)|$. Analyzing the maxima in the polarization difference $\Delta P(t)$ from Fig. 3(b), the relation $\Omega t_{\max}=1$ is found to hold well for the accessible range of pump frequencies. This indicates that the distribution of relaxation times is flat in the observed frequency regime. The full width at half maximum (FWHM) of the dielectric holes shown in Fig. 3(b) exceeds two decades for all pump frequencies.

The difference between the modified and the equilibrium responses cannot only be represented as ΔP, i.e., as the difference along the polarization axis. Another possibility is to monitor the difference along the time axis. In the following these time shifts are denoted as $\Delta(t)=\Delta\log_{10}(t/s)$. Due to the extreme stretching of the response functions, the maximum differences $\Delta_{\max}(t)$ are much larger than for supercooled liquids.[31] The difference $\Delta(t)$ has to be calculated at constant polarization $P(t)=P^*(t^*)$. Since for relaxors t^*

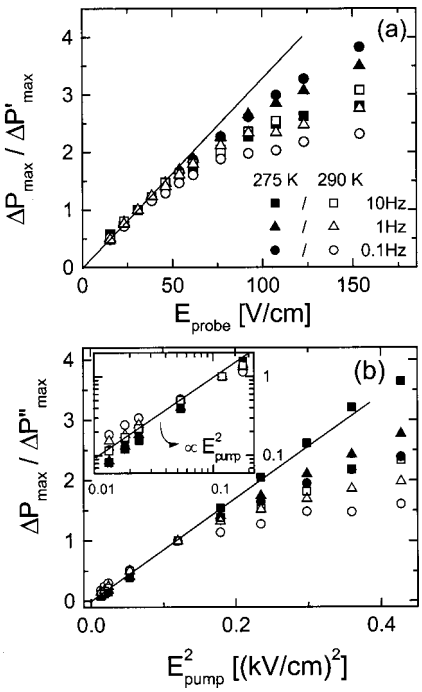

FIG. 4. (a) Maximum polarization modification ΔP_{max} plotted against the probe field for pump frequencies of 10, 1, and 0.1 Hz and temperatures of 275 K (full symbols) and 290 K (open symbols). The maximum modifications ΔP_{max} are normalized to $\Delta P'_{max}=\Delta P_{max}$ ($E_{probe}=30.8$ V/cm). (b) Dependence of ΔP_{max} on the square of the pump field for the same pump frequencies and temperatures as in (a). ΔP_{max} is normalized to $\Delta P''_{max}=\Delta P_{max}$ ($E_{pump}=346$ V/cm). The inset gives a double logarithmic presentation.

can differ from t by more than one decade [cf. Fig. 3(c)] the choice of a reference time is not unambiguous. Results of the difference $\Delta(t)$ with t as reference scale are shown in Fig. 3(c). Comparing these two representations one finds different shapes for $\Delta(t)$ and for $\Delta P(t)$. The curves for $\Delta(t)$ seem to be somewhat broader but the separation between the maxima also is about one decade in time for one decade difference in Ω. To explore $\Delta(t)$ more carefully it would be necessary to extend the time regime of the setup to both shorter and longer times. Therefore in the following we mainly present our data in terms of $\Delta P(t)$.

C. Variation of pump and probe fields

In order to avoid a modification of the polarization response by the probe field, E_{probe} had to be chosen much smaller than the pump field. Additionally the pump fields had to be chosen sufficiently large so that a detectable modification can be achieved. Figure 4 shows the dependence of the maximum polarization difference on the amplitude of (a) probe and (b) pump field for different frequencies and temperatures. It can be seen that ΔP_{max} evolves linearly in the probe field and quadratically in the pump field amplitude for sufficiently low voltages. The quadratic dependence of the pump fields suggests that the pump process is linear in the absorbed energy. This feature has also been observed in supercooled liquids,[31] spin glasses,[25] and ion conductors.[44] To simplify the interpretation the following measurements were always performed in the linear (E_{probe}) and the quadratic (E_{pump}) regime.

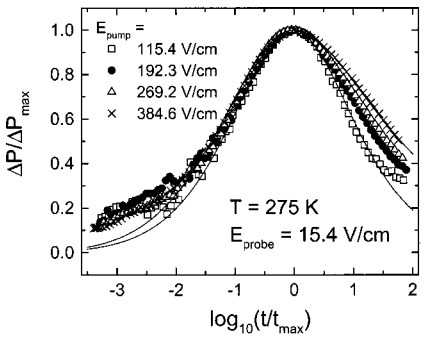

FIG. 5. Polarization modification ΔP for different pump fields and a pump frequency of 0.1 Hz. ΔP is normalized to the position of the maximum. The lines represent a fit to the data for the highest and the lowest pump field (see Sec. V).

The magnitude of the pump field amplitude slightly affects the shape of the holes. This can be seen from Fig. 5: the polarization differences from measurements for several amplitudes E_{pump}, of course all within the quadratic regime [Fig. 4(b)], are normalized to the amplitude of ΔP_{max} and to the time t_{max} at which the maximum in ΔP appears (t_{max} only slightly changes with E_{pump} but for a better analysis of the hole shape the curves in Fig. 5 are normalized to t_{max}). While the data for times shorter than t_{max} scale well onto each other this is not true for longer times. With larger pump fields the dielectric holes broaden somewhat.

D. Temperature dependence of the hole depths

Figure 6 shows ΔP_{max} for three different frequencies in the temperature range between 270 and 300 K. Around 300 K the maximum modifications exhibit no dependence on the pump frequency and are relatively small. For temperatures $T>300$ K ΔP is hardly detectable with our present setup. By lowering the temperature ΔP_{max} is increasing, then it peaks, and a strong frequency dispersion is observed. Below 270 K the time scales of the dipole reorientation times become

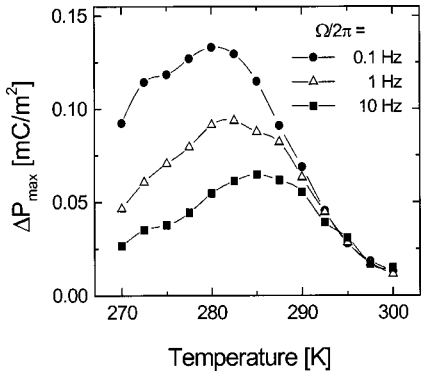

FIG. 6. Dependence of the maximum polarization modification ΔP_{max} on the temperature for pump frequencies of 10, 1, and 0.1 Hz.

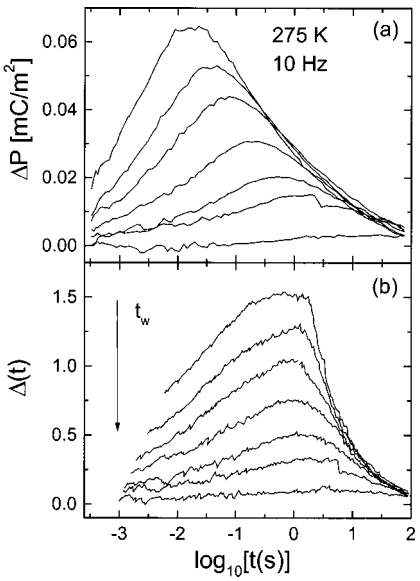

FIG. 7. (a) Polarization modification ΔP and (b) time difference $\Delta(t)$ for increasing waiting times $t_w/\mathrm{s}=0.001$, 0.003, 0.01, 0.03, 0.1, 0.3, 1, 10. The pump frequency was 10 Hz.

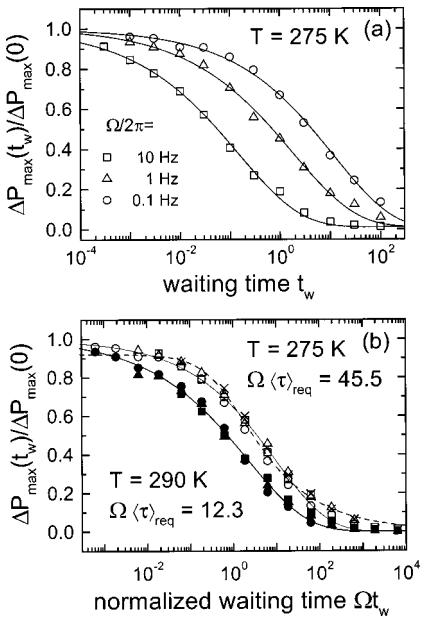

FIG. 8. (a) Normalized re-equilibration of $\Delta P_{\max}$ for pump frequencies of 10, 1, and 0.1 Hz at a temperature of 275 K. (b) The same data as in (a) and recovery data of the time difference $\Delta_{\max}(t_w)$ (crosses) are plotted against a normalized time axis Ωt_w. Also re-equilibration data for $T=290$ K are added (full symbols). The solid lines represent fits according Eq. (9), while the dotted ones follow Eq. (10).

much longer calling for repetition times between two subsequent field sequences of 600 s and more. Similar to the behavior of the complex dielectric constant for smaller values of the frequency the peak in $\Delta P_{\max}$ appears at lower temperatures. However, the frequency dispersion of $\Delta P_{\max}$ neither directly tracks the behavior of the dielectric permittivity nor that of the dielectric loss, or tan δ. It has to be recognized that within models for NHB other factors such as the specific heat[23,31] or the third-order nonlinear susceptibility[28] affect $\Delta P_{\max}$.

E. Re-equilibration of the dielectric holes

The data presented so far resulted from measurements employing a very short waiting time t_w between pump and probe procedure. By increasing this waiting time, one is able to monitor the re-equilibration (or recovery) of the dielectric holes.

We detected the temporal evolution of $\Delta P(t)$ [and likewise $\Delta(t)$] in PMN-10PT by increasing the waiting times from 1 ms up to 100 s. The results are depicted in Figs. 7(a) and (b) for a pump frequency of 10 Hz and a temperature of 275 K, respectively. Both diagrams show qualitatively the same features. The maxima in $\Delta P(t)$ as well as in $\Delta(t)$ decrease with increasing waiting time, i.e., after some time the system returns back to its initial state. In addition the maxima in $\Delta P(t)$ and $\Delta(t)$ shift to longer times during the re-equilibration. This effect appears more pronounced in the $\Delta P(t)$ representation. This can be interpreted to reflect the fact that differently relaxing subensembles contribute to the polarization response. Because the recovery for faster ensembles proceeds faster,[24] during the re-equilibration the fraction of slower ensembles contributing to ΔP increases.

Figure 8(a) shows the re-equilibration of $\Delta P_{\max}$ for three different frequencies at the same temperature. The time scale of this recovery strongly depends on the pump frequency. Shifting the pump frequency by one decade results in a recovery which also is shifted by about one decade. By plotting the normalized hole depths into one diagram with Ωt_w as the x axis, one can see that the re-equilibration curves for different frequencies superimpose. In Fig. 8(b) this is done for two different temperatures by analyzing data for $\Delta P(t)$ and $\Delta(t)$. Independent of the representation used for this analysis and of the burning frequency, the normalized data for $\Delta P_{\max}(t_w)$ as well as for $\Delta_{\max}(t_w)$ follow the same master curve.

It is seen that the re-equilibration of the holes for 290 K proceeds significantly faster than at 275 K. In order to analyze the refilling more precisely we used a stretched exponential function

$$\Delta P_{\max}(t_w)=\Delta P_{\max}(0)\exp[-(t_w/\tau_{\mathrm{req}})^{\beta}] \tag{9}$$

which provides a good fit to the data. The value of the exponent β turned out to be 0.36 ± 0.03 for the investigated temperature range. The average relaxation time $\langle\tau_{\mathrm{req}}\rangle=\beta^{-1}\Gamma(\beta^{-1})\tau_{\mathrm{req}}$ for 275 K is about 40 times longer than the intrinsic relaxation time $\tau_\Omega=\Omega^{-1}$ of those spectral contributions that have been affected most strongly by the pump process. Previously, this phenomenon was termed *long-lived dynamic heterogeneity*.[24]

We also fitted the data using a power-law function of the form

$$\Delta P_{\max}(t_w)=P_0\left(\frac{t_w+t_0}{t_0}\right)^{-\alpha}, \tag{10}$$

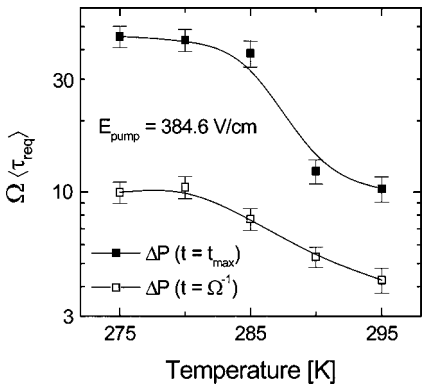

FIG. 9. Temperature dependence of the normalized re-equilibration time $\Omega\langle\tau_{\rm req}\rangle$ for the maximum polarization modification $\Delta P_{\rm max}$ (full symbols) and for ΔP at fixed times (open symbols). The lines are drawn to guide the eye.

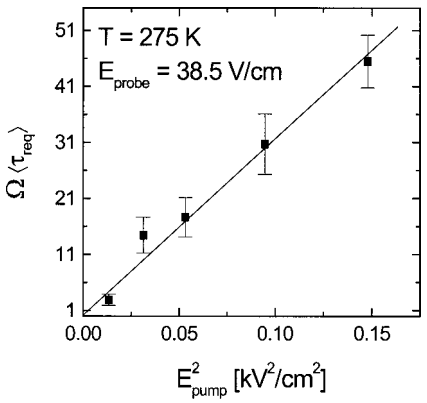

FIG. 10. Dependence of $\Omega\langle\tau_{\rm req}\rangle$ on the amplitude of the pump field at a temperature of 275 K. The line reflects a quadratic dependence of $\langle\tau_{\rm req}\rangle$ on the pump field.

which is often used to describe the t_w-dependent aging of dielectric or magnetic susceptibilities at a constant temperature. Initially the parameter t_0 has been introduced to take into account a possible delay of the beginning of aging.[41] In recent descriptions of measurements on the orientational glass $K_{1-x}Li_xTaO_3$ and on PMN-10PT t_0 was rather employed as a further parameter which determines the shape of the time trace of the aging quantity.[41,42] When fitting the data in Fig. 8(b) the parameter t_0 turned out to be 0.65 s at 275 K and 0.2 s at 290 K. The exponent α equals 0.36 ± 0.05 for all temperatures. A fit to the recovery data for 275 K is displayed in Fig. 8(b). While for shorter times the Kohlrausch function provides a superior fit, for longer times a power law according to Eq. (10) seems to be a somewhat better description.

Figure 9 shows recovery times determined at several temperatures in the range from 275 to 295 K. For each data point measurements from three pump frequencies were analyzed. Additionally, for 275 K $\Delta_{\rm max}(t_w)$ data were analyzed to extract the time scale of the recovery. The results show that $\langle\tau_{\rm req}\rangle$ is the same, irrespective of how it was determined. With increasing temperature $\langle\tau_{\rm req}\rangle$ becomes shorter but still exceeds τ_Ω significantly.

In addition, the recovery of the maximum polarization $\Delta P(t_w)$ at fixed times corresponding to the inverse pump frequency (i.e., at $t_\Omega=\Omega^{-1}$) has been analyzed. Figure 9 reveals that now one obtains shorter relaxation times than for the re-equilibration of $\Delta P_{\rm max}$. The data are also well fitted with Eq. (9). The stretching exponent β turned out to be slightly larger (0.42 ± 0.03) in comparison to that of the $\Delta P_{\rm max}$ data.

In Sec. II C we discussed the dependence of the shape of the dielectric holes on the pump field amplitude. In order to explore whether $\langle\tau_{\rm req}\rangle$ depends on the pump field we carried out several measurements with pump fields ranging from 115 to 384 V/cm. The result can be seen in Fig. 10. A significant dependence of the average recovery time on the pump field amplitude is observed. The results are compatible with a quadratic dependence of $\langle\tau_{\rm req}\rangle\propto E^2_{\rm pump}$.

V. DISCUSSION

As we will discuss in the following, the experimental results of nonresonant spectral hole burning help one to understand the dipolar dynamics of the disordered relaxor ferroelectric PMN-10PT in the observed temperature range $270<T<300$ K. This material shows strong spatial heterogeneities due to structural disorder.[6,7,29,43] The pronounced nonexponential decay of the polarization response (cf. Fig. 2) together with the frequency dependence of the polarization difference $\Delta P(t)$ as well as the time difference $\Delta(t)$ [see Figs. 3(b) and (c)] provide evidence also for a *dynamic heterogeneity* of the dipolar reorientation process. Depending on the frequency Ω of the energy input those parts of the spectrum are affected most that respond near Ω, so that $t_{\rm max}=\Omega^{-\alpha}$, with $\alpha\approx1$, is found for the accessible frequency range.[24] This provides evidence for an almost flat distribution of relaxation times existing in PMN-10PT in the observed frequency range. But it cannot definitely prove that a *purely heterogeneous* scenario is at the origin for the strong nonexponential behavior of PMN-10PT. As the following considerations reveal it is also possible that a superposition of intrinsic nonexponential processes leads to the observed dynamic behavior.

While in the ion-conducting glass CKN it has been observed that the spectral holes refill with a time constant $\tau_{\rm req}\approx\Omega^{-1}$,[44] in PMN-10PT the re-equilibration time $\tau_{\rm req}$ is significantly longer than the intrinsic relaxation time $\tau_\Omega=\Omega^{-1}$. In view of dielectric hole burning such a pronounced *long-lived heterogeneity* so far has only been observed in the slow β relaxation of glassy *D* sorbitol.[45] In addition, $\tau_{\rm req}$ strongly depends on the pump field amplitude and the temperature (see Figs. 9 and 10) while it scales with the pump frequencies, i.e., $\Omega\tau_{\rm req}$ is constant for each combination of pump field and temperature.

The observed pump field dependence of the re-equilibration can be understood *qualitatively* with reference to the change of the hole shape with the pump field amplitude (see Fig. 5). With increasing pump field an asymmetric broadening of the spectral holes is observed, i.e., for times shorter than the time $t_{\rm max}$ of the maximum modification the shape of the hole does not depend on the pump field while

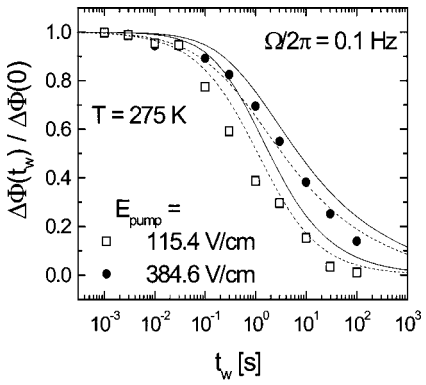

FIG. 11. Calculated re-equilibration function as described in the text for an exponential intrinsic relaxation (full line) and a Kohlrausch-like ($\beta=0.7$) intrinsic relaxation (dashed line). The symbols are the corresponding recovery data.

for longer times it does. Thus for large pump field amplitudes additional low-frequency spectral features affect the dielectric holes. As a consequence the lifetime of the hole becomes longer.

To analyze these features in more detail we performed calculations using the models described in Sec. II [see Eqs. (3a) and (3b)], with the constraint that the computed response function $\Delta\Phi$ fits the experimental data. To this end we took a sufficiently broad distribution of energy barriers $B(i)$ resulting in relaxation times $\tau_i=\tau_0\exp\{B(i)/k_BT\}$ so that the equilibrium response $\Phi(t)$ evolves logarithmically for times $-4<\log_{10}(t)<+3$. This exceeds our experimental time window [see Fig. 3(a)]. The pump process is associated with an absorption of energy ($\propto\varepsilon''$) in the material. In previous calculations we have used the Debye form for the dielectric loss.[23,31] However, in order to parameterize various shapes of spectral holes, here we will employ the imaginary part of the Havriliak Negami function, $\varepsilon''_{\mathrm{HN}}$,[46] on a trial basis. A calculation of $\Delta\Phi(t)$ with $f_{\mathrm{pump}}(\Omega,\tau_i)=\varepsilon''_{\mathrm{HN}}(\Omega,\tau_i)$ [Eqs. (3a) and (3b)] provides a good fit to the data, shown in Fig. 5 for the highest and the lowest pump field.

Using Eqs. (4)–(6) we calculated the recovery functions for several pump field amplitudes. Figure 11 shows the resulting recovery functions for two pump field amplitudes at a temperature of 275 K. They exhibit the same tendency as the corresponding recovery data: the re-equilibration time becomes longer when burning with a higher pump field.

Assuming a nonexponential intrinsic relaxation function for various quantities (Φ, Φ^*, and $\Delta T_{f,i}$) the hole shape for a given pump field can alternatively be fitted with a suitable $f_{\mathrm{pump}}(\Omega,\tau_i)$. The fits using the Kohlrausch form $\exp[-(t_w/\tau_i)^{\beta}]$ are as good as in the case of an intrinsic exponential relaxation (not shown). For a Kohlrausch β of 0.7 the exponent α (describing the shift of $t_{\max}$ with Ω, $t_{\max}=\Omega^{-\alpha}$) turned out to be 0.9. This is not significantly different from what the computations yield for $\beta=1$ ($\alpha=0.93$). But a difference arises in the hole recovery. For a Kohlrausch β of 0.7 the recovery becomes somewhat faster than for $\beta=1$ and is in semiquantitative agreement with the experimental data shown in Fig. 11.

The pump field dependence $\langle\tau_{\mathrm{req}}\rangle$ can at least qualitatively be explained with the model described above. However, the dependence on the temperature of the recovery times remains still unclear: While the width and the shape of the spectral holes does not change significantly (not shown) the recovery becomes shorter for higher temperatures (see Fig. 9). Furthermore the dependence of the hole depths on both the frequency (Fig. 3) and the temperature (Fig. 6) cannot be explained with the present model alone. To this end additionally the specific heat[23,31] or the third-order nonlinear susceptibility[28] may have to be regarded.

The model of an asymmetric double-well potential (see Sec. II) or a multiwell potential in a local random-field environment as outlined in Sec. II cannot explain the pump field dependence. Within these models the time scale of the recovery does not depend on the amplitude of the pump field. In the superparaelectric model[4] where polar regions are completely independent from their local environment flips of the polarization P occur in a multiwell potential which has several equilibrium states with equal energy. This scenario is ruled out since it does not exhibit any pump field dependent recovery. Recent calculations reveal that extrinsic relaxation mechanisms,[30] e.g., the mechanism related to domain-wall motion need to be involved in order to rationalize this finding.

One possible mechanism for the dipolar dynamics leading to a pump field dependence of the refilling rate is based on a scenario of ferroelectriclike nanodomains existing in PMN. This interpretation was proposed by Westphal *et al.*[13] and further developed by Glazounov and Tagantsev.[47,48] Structural defects in PMN and the influence of random fields originating from the random occupation of equivalent lattice sites by different ions can act as pinning centers for movable domain walls.[49] These pinning centers impede the growth of domains and lead to thermally activated motion of domain walls.[50] By applying a sufficiently large pump field not only can internal degrees of freedom within the domains be addressed but also certain domain-wall segments are released from their pinning centers. To recover, the domain walls again have to traverse back across the pinning barriers but now without the presence (and ''push'') of a pump field. This leads to a time scale of the re-equilibration τ_{req} that is longer than the intrinsic time scale Ω^{-1} set by the experiment. The notion of movable domain walls can also qualitatively rationalize the pump field and temperature dependence of τ_{req}. By increasing the pump field domain walls with increasingly large pinning energies can be released from their pinning centers. For those domain walls it takes longer time to re-equilibrate than for domain walls which have been addressed with lower pump fields.

The time scale $\langle\tau_{\mathrm{req}}\rangle$ shows a linear behavior in the absorbed energy, i.e., $\langle\tau_{\mathrm{req}}\rangle\propto E^2_{\mathrm{pump}}$ (Fig. 10). The temperature dependence of $\langle\tau_{\mathrm{req}}\rangle$ is shown in Fig. 9. For temperatures below 280 K the recovery time $\langle\tau_{\mathrm{req}}\rangle$ approaches a plateau value. For higher temperatures ($>$280 K) the time scale for recovery becomes significantly shorter. In view of the above interpretation this means that now enough thermal energy is provided to overcome the pinning barriers, i.e., the domain walls become more flexible. This results in a shorter re-equilibration time.

VI. CONCLUSION

We have demonstrated that nonresonant dielectric hole-burning is a useful tool to investigate dipolar reorientation processes in the relaxor ferroelectric material PMN-10PT. Frequency selective spectral holes can be burned into the polydispersive dielectric response with a maximum $\Delta P_{\max}$ appearing at a time corresponding to the inverse pump frequency Ω^{-1}. The re-equilibration of the spectral holes proceeds with a time constant τ_{req} significantly exceeding the intrinsic time of the pump process $\tau_{\Omega}=\Omega^{-1}$. The amplitude of the pump field determines how fast the spectral modification returns back to equilibrium. The field dependence for PMN-10PT revealed by the present study cannot be explained within a superparaelectric model or a model based on random fields against on-site reorientations. For the temperature range $270<T<300\,\mathrm{K}$ the interpretation favored to this end is a scenario of a ferroelectriclike state of polar nanodomains involving random fields. The walls of these domains can be pinned by defects or the random field environment in the relaxor material. In this scenario sufficient energy must be provided (by the pump field) to overcome the pinning barriers of the domain walls. This leads to a pump-field-dependent time constant of the recovery of the spectral holes.

ACKNOWLEDGMENTS

We thank the Deutsche Forschungsgemeinschaft (Grant No. Bo1304/4) for financial support, S. E. Park from the Material Research Laboratory (Pennsylvania State University) for generously providing the samples, and R. V. Chamberlin for fruitful discussions.

[1] G. A. Smolensky and A. I. Agronovskaya, Zh. Tekh. Fiz. **28**, 1491 (1958) [Sov. Phys. Tech. Phys. **3**, 1380 (1958)].
[2] T. R. Shrout and J. P. Dougherty, Ceram. Trans. **8**, 3 (1990), and references cited therein.
[3] K. Uchino, S. Nomura, L. E. Cross, R. E. Newnham, and S. J. Jang, J. Mater. Sci. **16**, 569 (1981).
[4] L. E. Cross, Ferroelectrics **76**, 241 (1987).
[5] L. E. Cross, Ferroelectrics **151**, 305 (1994).
[6] A. D. Hilton, D. J. Barber, C. A. Randall, and T. R. Shrout, J. Mater. Sci. **25**, 3461 (1990).
[7] L. A. Bursill, H. Qian, J. L. Peng, and X. D. Fan, Physica B **216**, 1 (1995).
[8] S. N. Dorogovtsev and N. K. Yushin, Ferroelectrics **112**, 27 (1990).
[9] D. Viehland, S. J. Jang, L. E. Cross, and M. Wuttig, J. Appl. Phys. **68**, 2916 (1990).
[10] E. V. Colla, E. Y. Koroleva, N. M. Okuneva, and S. B. Vakhrushev, J. Phys.: Condens. Matter **4**, 3671 (1992).
[11] K. Binder and A. P. Young, Rev. Mod. Phys. **58**, 801 (1986).
[12] U. T. Höchli, K. Knorr, and A. Loidl, Adv. Phys. **39**, 405 (1990).
[13] V. Westphal, W. Kleemann, and M. D. Glinchuck, Phys. Rev. Lett. **68**, 847 (1992).
[14] B. E. Vugmeister and H. Rabitz, Phys. Rev. B **57**, 7581 (1998).
[15] A. E. Glazounov and A. K. Tagantsev, J. Phys.: Condens. Matter **10**, 8863 (1998).
[16] R. Blinc, J. Dolinsek, A. Gregorovic, B. Zalar, C. Filipic, Z. Kutnjak, A. Levstik, and R. Pirc, Phys. Rev. Lett. **83**, 424 (1999).
[17] See, e.g., A. Hubert and R. Schäfer, *Magnetic Domains* (Springer, Berlin, 1998).
[18] T. Natterman, Y. Shapir, and I. Vilfan, Phys. Rev. B **42**, 8577 (1990), and references cited therein.
[19] K. H. Fisher and J. A. Hertz, *Spin Glasses* (Cambridge University Press, Cambridge, 1991); J. A. Mydosh, *Spin Glasses: An Experimental Introduction* (Taylor and Francis, London, 1993).
[20] A. K. Tagantsev and A. E. Glazounov, Appl. Phys. Lett. **74**, 1910 (1999).
[21] V. Bobnar, Z. Kutnjak, R. Pirc, R. Blinc, and A. Levstik, Phys. Rev. Lett. **84**, 5892 (2000).
[22] A. Levstik, Z. Kutnjak, C. Filipic, and R. Pirc, Phys. Rev. B **57**, 11 204 (1998).
[23] B. Schiener, R. Böhmer, A. Loidl, and R. V. Chamberlin, Science **274**, 752 (1996).
[24] O. Kircher, B. Schiener, and R. Böhmer, Phys. Rev. Lett. **81**, 4520 (1998).
[25] R. V. Chamberlin, Phys. Rev. Lett. **83**, 5134 (1999).
[26] W. Kleemann, V. Bobnar, J. Dec, P. Lehnen, R. Pankrath, and S. A. Prosandeev, Ferroelectrics (to be published).
[27] O. Kircher, R. V. Chamberlin, G. Diezemann, and R. Böhmer, J. Chem. Phys. **113**, 6449 (2000).
[28] R. Böhmer and G. Diezemann, in *Broadband Dielectric Spectroscopy*, edited by F. Kremer and A. Schönhals (Springer, Berlin, 2001).
[29] H. Qian and L. A. Bursill, Int. J. Mod. Phys. B **10**, 2007 (1996).
[30] G. Diezemann, Europhys. Lett. **53**, 604 (2001).
[31] B. Schiener, R. V. Chamberlin, G. Diezemann, and R. Böhmer, J. Chem. Phys. **107**, 7746 (1997).
[32] R. V. Chamberlin, Phys. Rev. Lett. **82**, 2520 (1999); see also R. V. Chamberlin, Nature (London) **408**, 337 (2000).
[33] R. V. Chamberlin, in *Liquid Dynamics*, edited by M. Fayer and J. Fourkas (American Chemical Society, Washington, DC, in press).
[34] I. M. Hodge, J. Non-Cryst. Solids **169**, 211 (1994).
[35] E. V. Colla, N. K. Yushin, and D. Viehland, J. Appl. Phys. **83**, 3298 (1998).
[36] Subsequent to thermal annealing we compared the shape of the modified polarization $\Delta P(t)$ as defined in Eq. (7) for identical experimental parameters from time to time but did not observe any changes. Also the temperature dependence of the broadband dielectric data (as presented in Fig. 1) did not show any difference after subsequent annealing procedures including several hole-burning measurements in between.
[37] A. Levstik, V. Bobnar, Z. Kutnjak, C. Filipic, and M. Kosec, J. Eur. Ceram. Soc. **19**, 1233 (1999).
[38] R. Richert, Rev. Sci. Instrum. **67**, 3217 (1996).
[39] Z.-Y. Cheng, R. S. Katiyar, X. Yao, and A. Guo, Phys. Rev. B **55**, 8165 (1997).

[40] R. Böhmer, B. Schiener, J. Hemberger, and R. V. Chamberlin, Z. Phys. B: Condens. Matter **99**, 91 (1995).
[41] F. Alberici, P. Doussineau, and A. Levelut, J. Phys. (France) **17**, 329 (1997).
[42] O. Kircher and R. Böhmer (unpublished).
[43] F. M. Jiang and S. Kojima, Appl. Phys. Lett. **77**, 1271 (2000).
[44] R. Richert and R. Böhmer, Phys. Rev. Lett. **83**, 4337 (1999).
[45] R. Richert, Europhys. Lett. (to be published).
[46] S. Havriliak and S. Negami, J. Polym. Sci., Part C: Polym. Symp. **14**, 99 (1966).
[47] A. E. Glazounov, A. K. Tagantsev, and A. J. Bell, Phys. Rev. B **53**, 11 281 (1996).
[48] A. K. Tagantsev and A. E. Glazounov, Phase Transitions **65**, 117 (1998).
[49] For recent reviews, see, e.g., D. S. Fisher, Phys. Rep. **301**, 113 (1998); H. Leschhorn, T. Nattermann, S. Stepanow, and L. H. Tang, Ann. Phys. (Leipzig) **6**, 1 (1997).
[50] T. Nattermann, Ferroelectrics **104**, 171 (1990).